A new algorithm for large surfaces profiling by fringe projection

S. Pavageau [a], R. Dallier [a], N. Servagent [a], T. Bosch [b,*]

[a] *Ecole des Mines de Nantes, 4 rue Alfred Kastler, BP 20722, 44307 Nantes Cedex 3, France*
[b] *ENSEEIHT-LEN7, Laboratoire d'Electronique, 2 rue Charles Camichel, BP 7122, 31071 Toulouse Cedex 7, France*

Abstract

A method for profiling surface objects based on the fringe projection method and a phase shifting algorithm is described. The application of this method to large surfaces is problematic since the calibration step requires the use of a reference plane as large as the object. A new algorithm based on least-squares method has also been developed to bypass this calibration step, and so the use of a reference plane. First experimental results on a carbon panel and on a parabolic aerial are presented to show the validity of the proposed algorithm. Accuracy of 1 mm has been obtained for an object of 1 m and 20 cm long, while sensitivity has been proved to be of the order of 100 μm.

Keywords: Fringe projection; Phase shifting; Profilometry; Object reconstruction

1. Introduction

Several optical methods exist, which can be employed for the determination of object shapes and profiles [1]. They have the advantages of being non-contact, and rapidly acquiring spatially dense data on large and small surfaces. This article presents a shape measurement method for large and flat surfaces based on the technique of fringe projection. This application forms part of an important stage of a wider research project (ALICE), dedicated to fundamental research in particle physics [2], and requires the building of a large detector system whose structural elements are carbon sandwich panels. Controlling the flatness of these large panels (2450 mm × 450 mm) is thus essential. The flatness, directly derived from the profile map is defined as the maximum distance between two perfect, parallel reference planes between which is placed the surface of interest. In order to guarantee relatively acceptable results from the whole fundamental experiment of the project ALICE, and according to conventional mechanical standard abacus, the flatness of these panels must be better than 150 $\mu m\,m^{-1}$.

The fringe projection method has been widely exploited for small object measurements [3]. However, due to some inherent calibration difficulties (principally the need for a reference plane as large as the object surface), relatively few published work have been reported on large area measurements using this method [4]. We report in this paper a new algorithm, based on least-squares method, which permits the profile of objects to be reconstructed with relative ease. The use of a physical reference plane is no more required. Theoretically, the algorithm may be applied for profiling objects of any arbitrary size. The theory and principles associated with our proposed method are thus discussed.

2. Fringe pattern analysis

Sinusoidal fringes are projected onto the object from one direction and viewed with a CCD camera from another direction (Fig. 1). These fringes are obtained by direct illumination of an optical grating and projected onto the object whose profile is to be determined. For object surfaces which are deformed, the phase of the projected fringes, and hence, their intensities are modulated accordingly.

This resulting intensity distribution is then recorded by the CCD camera and can be given by the following expression:

$$I(x, y) = a(x, y) + b(x, y)\cos[\phi(x, y)] \quad (1)$$

where $a(x, y)$ and $b(x, y)$ are the fringe pattern average and modulation intensities and $\phi(x, y)$ is the phase containing the surface relief deformation.

To extract the phase $\phi(x, y)$ from the intensity distribution, we use a phase shifting method, where the phase is calculated for each pixel.

* Corresponding author. Tel.: +33-561-588-282; fax: +33-561-588-237.
E-mail address: bosch@len7.enseeiht.fr (T. Bosch).

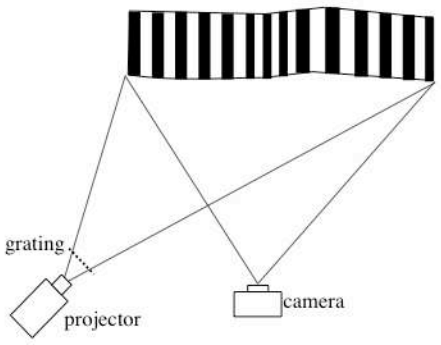

Fig. 1. Scheme of fringe projection.

To determine the phase, several consecutive sets of fringes, each with a constant and pre-determined phase-shift, are projected onto the object. Among the various algorithms available, we have chosen to work with the windowed discrete Fourier transform (WDFT) [5]. The main reason is its relative insensitivity to a linear phase-shift miscalibration. This algorithm is also insensitive to bias modulation of the fringe pattern due to non-uniform illumination. The WDFT algorithm is given by the following expression:

$$\phi(x,y) = \arctan\left[-\frac{\sum_{k=1}^{N-1} k(I_{k-1}(x,y) - I_{2N-k-1}(x,y))\sin(2k\pi/N)}{NI_{N-1} + \sum_{k=1}^{N-1} k(I_{k-1}(x,y) + I_{2N-k-1}(x,y))\cos(2k\pi/N)}\right] \quad (2)$$

where I_k is the kth fringe intensity recorded and $\delta = 2\pi/N$ is the phase-shift. $\phi(x, y)$ lies within the range $[-\pi, \pi]$.

The 2π phase jump, introduced by the "arctan" term, must be removed by the process known as phase unwrapping to recover the surface heights [6]. This process consists of adding or subtracting an adequate multiple of 2π. The result of this process is a phase map, given by a continuous two-dimensional phase variation of the object surface.

The phase map is then processed to give a set of depth information from which the desired object profile and flatness can be obtained. For small objects, a physical reference plane is used to calibrate the setup and a simple relationship can be found between the object profile and the phase map. However, this method is no longer applicable to objects of larger dimensions. Section 3 describes the technique we have employed to profile large object surfaces.

3. Reconstruction algorithm

To obtain the shape of an object from the given phase map, we consider the complete theoretical approach. We also define an exact transformation relating each point on the original grating (known as projector reference) to their respective image points as observed by the camera (receiver reference). This transformation is determined by assuming a virtual plane object surface and leads to a theoretical phase expression (ϕ_{th}). This in turn results in an expression for the height variation (z_{th}) of this object. Each expression depends on the associated geometrical parameters of the experimental setup (magnifications, grating pitch, distances between the three reference planes: object–projection planes

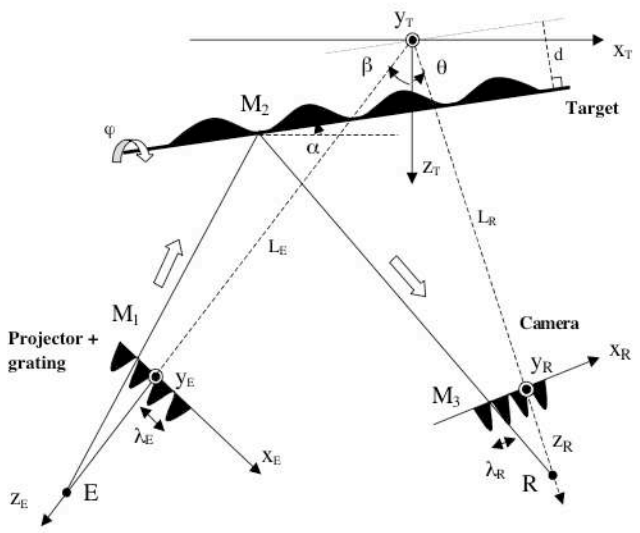

Fig. 2. Optical geometry of the setup.

and object–receiver planes, projection and receiving angles), as well as those of the object itself (α, φ, d, corresponding to object angle with respect to the horizontal, the object tilt angle and the distance from the reference origin, respectively). Fig. 2 shows the optical geometry of the setup.

Assuming that the above parameters are known, we can then calculate the height variation and the profile of the object. The former parameters can be estimated with reasonable ease. Although the geometrical parameters of the object are not easily available from direct measurements, they can, however, be inferred from the unwrapped phase. In order to do this, the object surface is divided into many equal elementary planes P_i, where i represents the ith plane. Since only three points, A_i, B_i, C_i suffice mathematically for the description of a plane, the theoretical phase and height variation expressions for each individual point can therefore be solely determined by the three unknown parameters (α, φ, d as described earlier). To obtain a good estimate of the above parameters for each plane, we have adopted the following procedure:

1. Define three starting unknowns: α_0, φ_0 and d_0.
2. Then calculate the theoretical phases for the three points A_i, B_i, C_i, given by $\phi_{th_{A_i}}(\alpha_0, \varphi_0, d_0)$, $\phi_{th_{B_i}}(\alpha_0, \varphi_0, d_0)$, $\phi_{th_{C_i}}(\alpha_0, \varphi_0, d_0)$, respectively.
3. Obtain the experimental phases of the three points, given by $\phi_{exp_{A_i}}$, $\phi_{exp_{B_i}}$ and $\phi_{exp_{C_i}}$, from the phase shifting and unwrapping schemes.
4. The parameters α_i, φ_i and d_i, for a plane P_i, can then be found by fulfilling the below conditions:

$$\phi_{\exp_{A_i}} = \phi_{\mathrm{th}_{A_i}} \qquad \phi_{\exp_{B_i}} = \phi_{\mathrm{th}_{B_i}} \qquad \phi_{\exp_{C_i}} = \phi_{\mathrm{th}_{C_i}} \quad (3)$$

5. Concretely, in order to achieve the best possible approximation of the parameters, we exploited a minimizing function given by

$$F(\alpha, \varphi, d) = |\phi_{\mathrm{th}_A}(\alpha, \varphi, d) - \phi_{\exp_A}|^2 + |\phi_{\mathrm{th}_B}(\alpha, \varphi, d) - \phi_{\exp_B}|^2 + |\phi_{\mathrm{th}_C}(\alpha, \varphi, d) - \phi_{\exp_C}|^2 \quad (4)$$

where $\phi_{\exp_A}$, $\phi_{\exp_B}$, $\phi_{\exp_C}$ are the measured phases at points A, B, C, respectively, during fringe projection and ϕ_{th_A}, ϕ_{th_B} and ϕ_{th_C} are the corresponding calculated phases.

The surface height for an individual plane, z_i, can thus be calculated as a function of the geometrical parameters, α_i, φ_i and d_i. Subsequently, the height values for other elementary planes, $z_{i+1}, \ldots, z_{i+n}$, can be similarly calculated. The entire surface profile of the object can finally be reconstituted from the calculated heights of all elementary planes.

In the following sections, the first experimental results will be presented to show the validity of our algorithm.

Processing of the acquired data is carried out via a program written in Matlab®.

4. Experimental results

The configuration of the experimental setup is illustrated in Fig. 2. The projector, which has been built in our laboratory, consists of a tungsten–halogen lamp illuminating a grating to allow projection of the fringes on the object under test. A sinusoidal grating with a pitch of 0.2 mm has been employed. It is translated using a motorized translation stage controlled by a program written in Labview® to produce the desired phase-shift.

In order to correctly calculate the phase map, seven intensity maps obtained by the phase shifting technique are recorded. Note that a phase-shift of $\pi/2$ has been introduced between each intensity map (corresponding to a 50 μm transverse displacement of the grating in this case). This phase-shift is considered to be relatively constant since each motor step is only 15 nm. Moreover, as previously mentioned, the WDFT algorithm used for phase determination is relatively insensitive to any phase mismatch.

The deformed fringe patterns on the object surface are next captured by a CCD camera (1035 × 1317 pixels, 12 bits coding).

The projector is located at a distance $L_E \approx 6$ m from the object with a measured projection angle of 38.75° while the camera has been positioned at $L_R = 4.5$ m with a receiving angle of 23.25°. By exploiting this configuration, a field of view of ≈1.2 m in length can be visualized.

4.1. Carbon panel

The setup has been first developed to verify the flatness of black carbon panels of large dimensions (up to 2450 mm × 450 mm). The carbon panels have to be held vertically, in order to overcome the problem of deformation under their own weight. A system of three contact points was used for this purpose. A preliminary test was realized on a 1250 mm × 450 mm carbon panel and its resulting 3D contour map is shown in Fig. 3. A peak-to-valley distance of approximately 1 mm has been obtained.

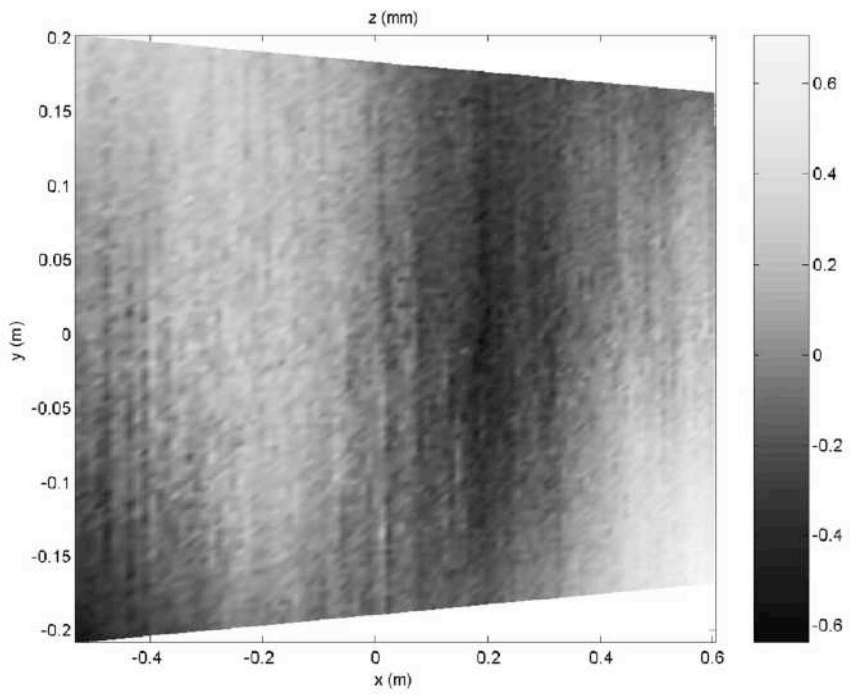

Fig. 3. 3D contour map of a 1250 × 450 carbon panel (scale in mm; the trapezoidal form is due to perspective correction).

The same panel was also tested with an opto-mechanical setup we have previously developed [7], where a peak-to-valley distance of 150 μm has been found. This last measurement can be considered as a reference.

The discrepancies between the two measurements can be explained as follows. In fact, the profile obtained using structured light projection principally results from imperfections in the imaging system (optical distortion). Indeed, during simulations, where no optical distortion was introduced, the influence of the geometrical parameters (introduced errors of 1 cm for L_E, L_R, 1° for $\beta, \theta, \ldots$) was found to be negligible. However, in practice, optical distortion exists and leads to degradations of the measurement accuracy. This is the main source of uncertainties in our setup. Note that we have used a seven-lens, commercial videoprojection objective, whose optical imperfections cannot be easily calculated nor measured. An improvement of the projection system would then be the design of a dedicated and completely known optical system, although this constitutes an expensive solution.

Currently, with the systematic warp of 1 mm, which degrades the accuracy of the setup, it is impossible to map the carbon panels and so, to measure their flatness. However the sensitivity of the setup has been demonstrated by carrying out relative measurements. By relative measurement, we means that we subtract this warp whose profile is given in Fig. 3 from each newly reconstructed object profile.

To illustrate the results from these measurements, we placed an A3 size sheet of paper on the same panel. The paper thickness has been estimated to be 110 ± 10 μm using a vernier caliper. A new set of seven images are next recorded. Finally, the profile of the panel is subtracted from the obtained profile incorporating the sheet of paper. Fig. 4 shows the 3D reconstruction of the paper thickness. The calculated thickness, taking into account both the paper itself as well as the fine film of adhesive used (≈20 μm), is approximately 155 μm.

Most importantly, Fig. 4 illustrates that the system can be employed to resolve details of ≈150 μm in height within a large observation field of 1200 mm × 450 mm. In addition, measurements can be considered as highly repeatable, since a reference set of data can be subtracted, at a later time, from images taken under the same conditions.

4.2. Elliptic paraboloid

In the first example, our algorithm is used on the flatness measurement of carbon panel, which length is more than 1 m. However, our proposed algorithm is not only restricted to the determination of planar objects. Its application can be extended to the measurement of smaller surfaces as well as large and non-planar surfaces (without shadow zone). For example, the algorithm has been tested on a parabolic aerial. The aerial is a 850 mm × 950 mm elliptic paraboloid, white and mat, 80 ± 1 mm height and is held vertically by a aluminum support. The same setup configuration (angle, distance, etc.) as for carbon panel is kept. This implies an accuracy of measurements of 1 mm.

Fig. 5 shows the reconstituted 3D contour map of the elliptic paraboloid. To point out the robustness of the algorithm, a cross-section profile of the paraboloid, passing through its top is given in Fig. 6. A height of 79 mm is obtained.

Repeatability tests have also been carried out. About ten sets of seven images have thus been recorded on the same paraboloid. The histogram shown in Fig. 7

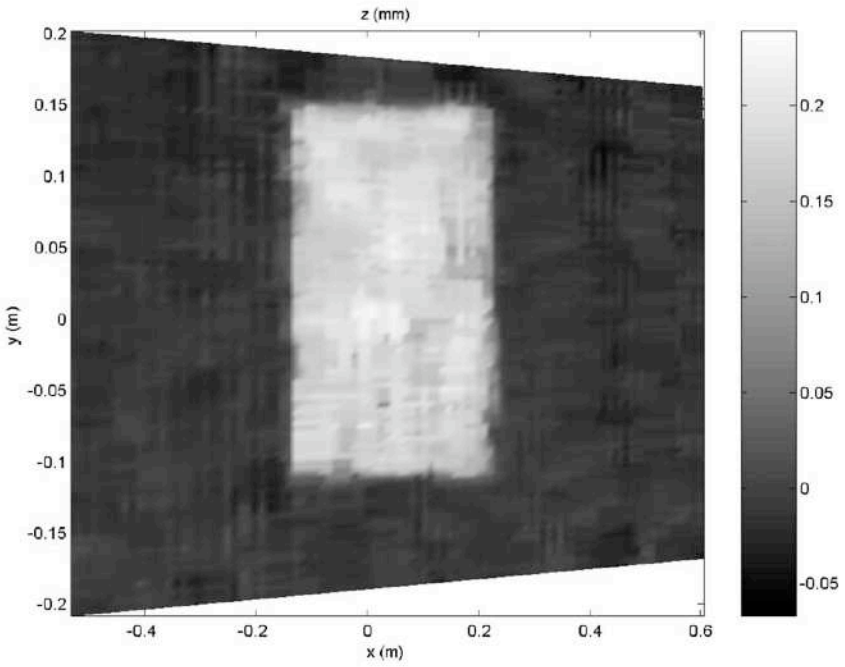

Fig. 4. 3D reconstruction of the paper thickness (scale in mm).

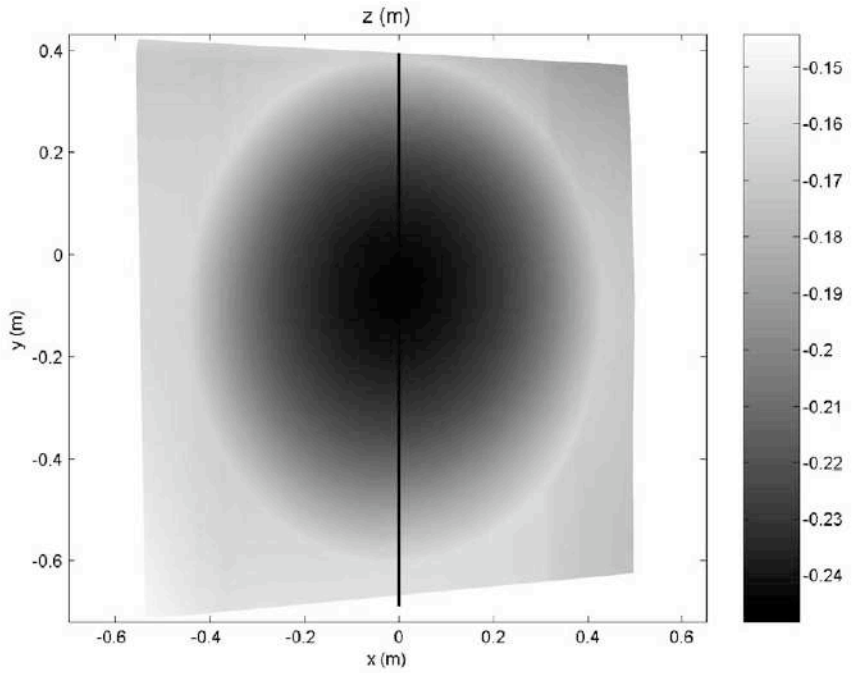

Fig. 5. 3D contour map of an elliptic paraboloid (scale in m; the trapezoidal form is due to perspective correction).

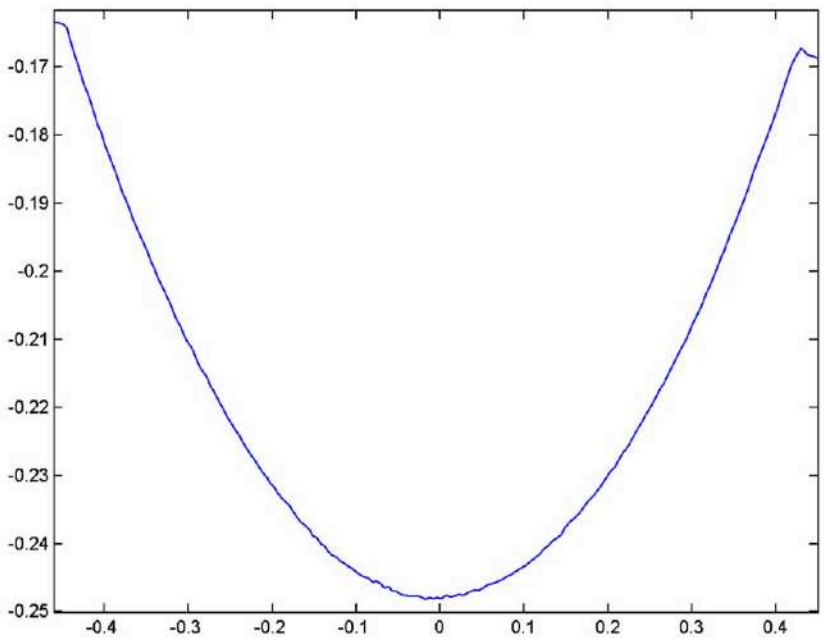

Fig. 6. A cross-section profile of the paraboloid ($x = 0$).

represents the distribution of the measurements around mean value. The experimental results present an uncertainty of $\pm 200\,\mu$m, interval corresponding to 95% of the measurements. Our setup can be considered as highly repeatable.

These first results are quite encouraging concerning the feasibility of the algorithm we have developed. However, further improvements are needed to reduce errors which degrade the measurement accuracy. One of the improvements would be to reduce lens distortions of the imaging system. In fact, the distortions lead to an error on the projection of the fringes and so on the measurement of the experimental phase. Reducing the distortion would decrease the uncertainty on the experimental phase. Improvement on the camera model used (optical distortion, etc.) as well as the evaluation of the influence of the setup parameters would lead to

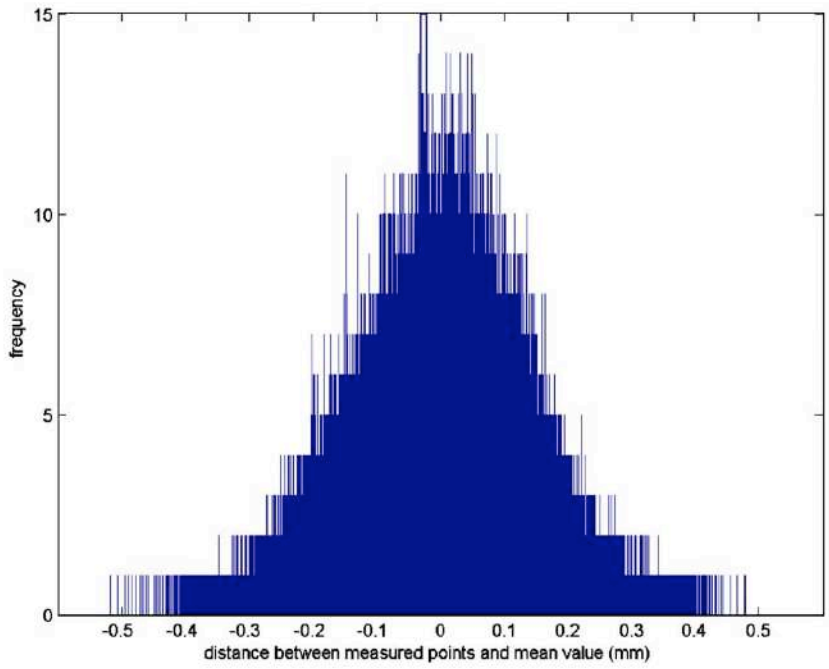

Fig. 7. Distribution histogram of distance measurement on a paraboloid.

a better determination of the theoretical phase and increase the accuracy.

5. Conclusion

This paper presents a method for full-field shape measurements on large surfaces by exploiting structured light projection. It is non-contact, rapid and can be easily automated. The algorithm that we have reported here in this work, was firstly developed for relatively flat surfaces. It does not require any cumbersome calibration procedures and its principal advantages are the absence of a physical reference plane and that it can be applied on all surfaces (small, large, planar and non-planar). First experiments were carried out on 1250 mm × 450 mm carbon panel and on a parabolic aerial. Unfortunately, optical distortions degrade the accuracy of the measurements, which is currently, approximately 1 mm. This prototype could be easily adapted to specific needs such as, in aerospace, automotive or shipbuilding industry.

References

[1] F. Chen, G.M. Brown, M. Song, Overview of three-dimensional shape measurement using optical methods, Opt. Eng. 39 (2000) 10–22.
[2] ALICE collaboration, Dimuon forward spectrometer: technical design report, CERN/LHC 2000-046, addendum 1, 2000.
[3] C. Quan, X.Y. He, C.F. Wang, C.J. Tay, H.M. Shang, Shape measurement of small objects using LCD fringe projection with phase shifting, Opt. Commun. 189 (2001) 21–29.
[4] M. Lehmann, P. Jacquot, M. Facchini, Shape measurements on large surfaces by fringe projection, Exp. Tech. 23 (1999) 31–35.
[5] Y. Surrel, Fringe analysis, Photomechanics, Springer, Berlin, 1999, pp. 55–102.
[6] D.C. Ghiglia, M.D. Pritt, Two-dimensional Phase Unwrapping: Theory, Algorithms and Software, Wiley, New York, 1998.
[7] S. Pavageau, R. Dallier, N. Servagent, T. Bosch, High accuracy optical measurement of flatness for large object, Meas. Sci. Technol. 14 (2003) 2121–2126.